

Article

The Laser Scanner Technique: A Tool for Determining Shear Strength Parameters of Rock Mass Discontinuities

Margherita Zimbardo ¹, Alessandra Nocilla ^{2,*}  and Anna Scotto di Santolo ¹

¹ Faculty of Engineering and Computer Science, Telematic University Pegaso, 80143 Napoli, Italy; margherita.zimbardo@unipegaso.it (M.Z.); anna.scottodisantolo@unipegaso.it (A.S.d.S.)

² Department Civil, Environmental, Architectural Engineering and Mathematics (DICATAM), University of Brescia, 25123 Brescia, Italy

* Correspondence: alessandra.nocilla@unibs.it

Abstract: When evaluating the shear strength of rock mass discontinuities, certain challenges arise due to the difficulty in quantifying the roughness characteristics of surfaces and the strength of asperities. Recent research has focused on enhancing techniques for assessing these characteristics and exploring the application of laser scanning to aid in evaluating discontinuity features. The analysis of reflectivity values (I) obtained through a laser scanner survey presents an efficient method for assessing mechanical characteristics, such as joint compressive strength (JCS). Reflectivity measurements demonstrate correlations with Schmidt hammer rebound values (r). The laser scanner technique would enable the measurement of JCS without the direct application of the Schmidt hammer on rocks in areas where rebound values (r) measurements are unavailable. The use of a laser scanner allows for the acquisition of high-precision geometrical information concerning the 3D roughness and anisotropy of rock surfaces. In this study, an innovative technique was introduced that utilizes laser scanner data from six previous experimental surveys conducted on rock formations in Southern Italy. This technique facilitates the evaluation of roughness profiles, considering potential variations along kinematically admissible sliding directions, allowing for the estimation of the Joint Roughness Coefficient (JRC). This new methodology aids in evaluating the parameters of Barton's equation to determine the strength characteristics of rock mass discontinuities.

Keywords: laser scanner; rock mass; discontinuity shear strength; JCS ; JRC ; reflectivity; roughness profiles



Citation: Zimbardo, M.; Nocilla, A.; Scotto di Santolo, A. The Laser Scanner Technique: A Tool for Determining Shear Strength Parameters of Rock Mass Discontinuities. *Appl. Sci.* **2024**, *14*, 5793. <https://doi.org/10.3390/app14135793>

Academic Editor: Tiago Miranda

Received: 13 May 2024

Revised: 14 June 2024

Accepted: 20 June 2024

Published: 2 July 2024



Copyright: © 2024 by the authors. Licensee MDPI, Basel, Switzerland. This article is an open access article distributed under the terms and conditions of the Creative Commons Attribution (CC BY) license (<https://creativecommons.org/licenses/by/4.0/>).

1. Introduction

1.1. Laser Scanner: Geometric Characterisation of Rock Mass Discontinuities

The laser scanning survey is a well-established methodology for assessing the oriented structure of a rock mass and the parameters that geometrically describe it, including orientation, persistence, spacing of discontinuities, and degree of fracturing [1,2]. This technique goes beyond the conventional definition of the three-dimensional model of the slope. It serves as an efficient method for digitizing and modeling a rock mass [3].

On-site survey enables the measurement of geometric quantities such as orientation, spacing, and persistence of discontinuities. This information allows for assessments of the degree of mass fracturing and the size of the blocks that may form. These assessments can be conducted either deterministically or statistically, depending on the representativeness of the collected data sample [4].

The introduction of indirect close-range methods enables the generation of a Digital Terrain Model (DTM) for the specific wall. Using appropriate software tools, measurements of the orientation of discontinuities can be directly conducted on the digital model [5,6].

With LIDAR (Laser Imaging Detection and Ranging) technology, the polar coordinates of points are acquired based on a reference system with the origin at the center of the instrument. In rock mechanics, the scanners typically used have an acquisition

range that varies between 100 and 1000m, with scanning speeds ranging from 2000 to 100,000 points per second. The analysis aimed at determining the discontinuity planes and their orientation can be carried out either manually or automatically on the Digital Terrain Model (DTM) [7]. In the first case, the operator manually selects, for each plane, a sufficient number of points to determine its orientation, including dip and dip direction. The second option relies on an automated approach to extract discontinuity planes from a dense Digital Surface Model (DSM) of a rock face obtained through laser scanning and computes their parameters [4,8].

There are several software applications that perform the tasks of detecting planes and determining their equations. These software tools essentially differ in the algorithms they implement. The simpler ones are limited to determining the plane equations using the least squares method applied to points subjectively selected by the operator. More sophisticated methods are based on segmentation algorithms capable of identifying different planes within the point cloud, as well as detecting and automatically removing outliers. [9].

1.2. Laser Scanner: Mechanical Characterisation of Rock Mass Discontinuities

The mechanical properties of discontinuities are of primary importance, as they largely influence the mechanical behavior of the rock mass. Fast and reliable field measurements of the strength properties of rock hold significant practical importance in rock engineering [10,11]. Many authors have proposed new techniques to predict the strength parameters of rock mass [12–14].

The superficial portion of any rocky material exhibits lower strength characteristics compared to those measured within the intact rock due to physical and chemical weathering processes that propagate internally with progression [15].

These processes depend on the porosity of the material and the presence of micro-cracks or micro-fractures of varying extent. Even minor weathering can lead to a decline in rock strength, specifically joint compressive strength (*JCS*), which primarily occurs along discontinuity surfaces in outcrops. This characteristic can be measured in the laboratory through direct shear tests on samples taken from the joints. However, the difficulty in its determination is often influenced by textural anisotropy and the inability to obtain representative samples, especially in the presence of large-scale variations. Indirect tests, such as estimation using the Schmidt hammer and point load tests, are commonly employed to estimate the *JCS*. The Schmidt hammer rebound hardness test, developed in 1948, is a straightforward and non-destructive method initially designed for a rapid assessment of Uniaxial Compressive Strength (*UCS*) [16].

Over time, it has been further adapted to gauge the hardness and strength of rock [17,18]. The recorded rebound height of the mass (*r*) on a linear scale provides insight into the strength characteristics of the tested material. The most recent research suggests that a new technique based on the use of laser scanning may allow assessment of characteristics such as the status of surface discontinuities, which is known to affect the shear strength of discontinuities. Assessing the ratio between the energy of the reflected ray and the one emitted by the instrument, called “reflectivity (*I*),” makes it possible to obtain information on rock surface characteristics. The property of any surface to reflect electromagnetic radiation depending on its nature has suggested using this characteristic for assessments of the physical and mechanical parameters of materials. For example, through the digital processing of images and reflectivity values obtained from laser scans, it has been possible to correlate reflectivity with the content of clay minerals in rocks [19,20].

The reflectivity depends on the characteristics of the material constituting the surface under survey and the wavelength of the light signal. The reflectivity recorded during the scan could, therefore, provide information about the textural characteristics (micro-fractures, micro-roughness, porosity, alteration) of the rock and the decay of lithic materials. Each element of the terrain reflects, absorbs, or transmits incident energy at different wavelengths, depending on its chemical–physical and structural characteristics (spectral signature). These considerations form the basis of techniques developed for recognizing

surfaces using methods typical of remote sensing. If it is possible to explore, at various wavelengths, the light reflected from a surface and there is a sufficiently extensive statistical record of spectral behavior, it is then possible to identify the nature of the investigated object [21].

The spectral reflectance of terrains is primarily controlled by water content, organic matter content, grain size, iron oxide content, mineralogy, and structure [22,23].

The comparison between the spectral signatures of known soils and/or reference minerals allows for qualitative assessments of the properties of soils that have not been investigated yet [24,25]. The software accompanying the scanner displays the scan results and encodes the reflectivity of surfaces with values indicated by a DN (Digital Number) ranging from 0 to 255. A value of 0 corresponds to zero reflectance, referring to bodies that completely absorb the laser beam without reflecting it, such as black bodies, while the value 255 indicates maximum reflectance.

1.3. Laser Scanner: Roughness Characterisation of Rock Mass Discontinuities

The morphology of surfaces, quantified by Barton [26] using the Joint Roughness Coefficient (*JRC*), is one of the characteristics that governs the shear strength of discontinuities. In situ, it is typically assessed by measuring one or two profiles of the discontinuities in a specified direction with a profilometer, with dimensions typically no greater than 30–40 cm, and comparing the obtained profile to typical profiles proposed by Barton and ISRM. Roughness parameters of rock joints are scaledependent, and their descriptors change with scale [27]. Obtaining an estimation of the roughness of a rock joint contributes to a better understanding of the failure mechanism and permeability characteristics of a rock mass [28]. *JRC* is a parameter significantly influenced by the scale effect, which can be taken into account by adopting the precautionary expression (1) provided by Barton and Bandis [29].

$$\tau = \sigma_n \tan \left[\varphi_r + JRC \log_{10} \left(\frac{JCS}{\sigma_n} \right) \right] \quad (1)$$

The authors developed the Barton–Bandis (BB) model using *JRC* and Joint Wall Compressive Strength (*JCS*) and highlighted the importance of the scale effect. Many researchers improved the evaluation of *JRC* by developing new methods and new parameters (i.e., the micro-average inclination angle, the roughness profile index—*Rp*, fractal dimension) [30–36].

However, these methods do not consider the anisotropy of the surfaces, which is also a function of the genesis of the discontinuities [37]. The measurement of joint roughness is increasingly attracting attention with the growing prevalence of high-performance computing and non-contact measurement techniques. Techniques such as photogrammetry, image processing, structured-light scanning, and laser scanning offer effective solutions for estimating Joint Roughness Coefficient (*JRC*) based on roughness measurements. The laser scanning method for assessing surface roughness relies on utilizing lasers to measure the distance to an object based on the speed of light [27,38,39].

High-precision information can be obtained through the use of laser scanning in the laboratory regarding the 3D roughness and anisotropy of discontinuity surfaces [40–44]. This has allowed for new and more refined formulations of the peak shear strength expression for rough discontinuities, overcoming the limitations associated with profilometer-based survey techniques typically performed on individual sections oriented along predetermined directions [45–47]. The laser scanner technique can also be extended to field surveys and could allow for the measurement of roughness profiles as the direction of kinematically admissible sliding varies, thus providing valuable information for the assessment of the Joint Roughness Coefficient (*JRC*) on a larger scale. According to Bao et al. [48], the sampling intervals of profile lines and digital points both affect the calculated *JRC* values. The laser scanning technique can overcome these limitations, allowing the evaluation of the anisotropy of roughness. The laser scanner survey enables a quick assessment of the rock mass quality [49,50].

This research has focused on the use of laser scanning technology for the survey of rock mass discontinuities to determine the Barton parameters (JRC and JCS) necessary for assessing the shear strength of the discontinuity surfaces. The utilization of a laser scanner enables the acquisition of high-precision geometrical information regarding the 3D roughness (JRC) and its anisotropy of rock mass discontinuity and the measurement of JCS without the direct application of the Schmidt hammer on rocks. The objective pursued was to indirectly assess the in situ strength of the rock by measuring the degree of alteration through the differing emissivity of the surface when hit by a laser beam, depending on the surface's microstructure [51]. The technique was developed on stone materials of different lithology and varying degrees of alteration on which it was possible to perform both laser scanner surveys (from which reflectivity values, I , were acquired) and direct measurements of the rebound value (r) with the Schmidt hammer to assess the possibility of correlating spectral reflectance with the joint compressive strength (JCS) parameter. The determination of both Barton parameters through the same technique represents a motivating goal of the research.

2. Materials and Methods

A new perspective is presented in this study, introducing a new methodology for evaluating the parameters of Barton's equation (JCS and JCR) in determining the strength characteristics of discontinuities within the rock mass. The two parameters are essential for the mechanical characterization of mass discontinuities, and acquiring them on extensive outcrops and numerous discontinuities could allow a reliable assessment of scale effects in relation to the direction of imposed displacements, as well as a statistical evaluation. The objective of the research, evaluating data obtained from six surveys and previous research, was therefore to verify the possibility of using laser techniques for rock alteration and its strength (JCS) and surveys of roughness (JRC).

Compared to intact rock, discontinuity surfaces within the rock mass generally exhibit lower strength characteristics due to physico-chemical weathering processes. Even a moderate degree of weathering, primarily occurring on the surfaces of the discontinuities in exposed rock masses, is sufficient to cause a decrease in rock strength (i.e., Joint Coefficient of Strength— JCS). The assessment of rock strength can be conducted in the laboratory through direct shear tests on samples extracted from joints. However, the challenge in determining this strength often arises from textural anisotropy and the difficulty of obtaining representative samples, especially in the presence of significant large-scale variations. To compare data from manual investigations and laser surveys, information was collected on various discontinuities using both the Schmidt hammer (Original Schmidt—Type L-9 Impact energy: 0.735 Nm, piston diameter: 15 mm, Kolida Instrument Picerno, Italy) and laser scanning techniques. According to ISRM recommendations, 10 rebound values (corresponding to the relative JCS according to the linear correlation proposed for the Schmidt hammer) were measured directly on site for each discontinuity.

The value of JCS (joint compressive strength) can then be determined using the diagram (Figure 1) proposed by Deere and Miller [52]. In this diagram, various Schmidt indices are plotted along the x -axis as the hammer inclination varies, while JCS values are indicated on the y -axis. To determine the JCS value, it is necessary to use one of the inclined lines present in the diagram, selected based on the unit weight of the rock under examination.

Simultaneously, on the same surface, the laser survey recorded reflectivity values (i.e., 30 digital numerical values for each discontinuity). The laser scanner is indeed capable of measuring the values of incident and reflected beam energy, providing the corresponding reflectivity ratio (I).

This present study has focused on correlating rebound values (r) measured directly with the Schmidt hammer (i.e., traditional direct techniques) and reflectivity values (I) obtained through laser scanning surveys for the same surfaces. In Table 1, the identifying names of the investigation sites, the present lithotype, the type of laser scanner used,

whether the measurement of reflectivity and rebound with the Schmidt hammer was obtained, and whether the surface roughness (*JRC*) was also determined, are reported.

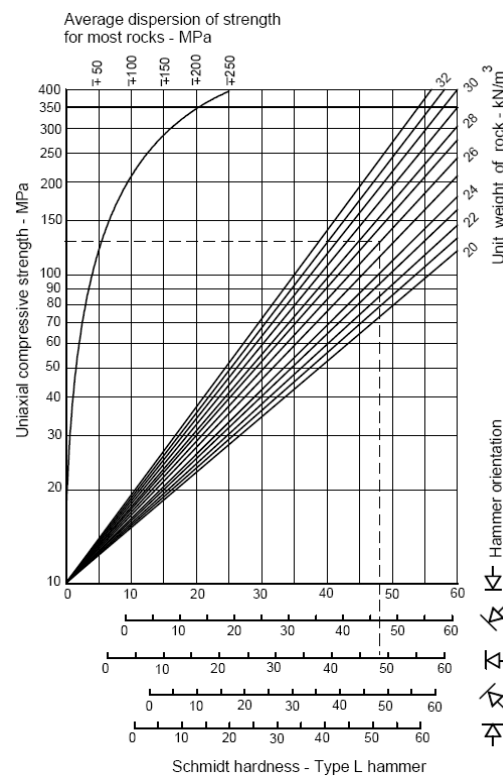


Figure 1. Schmidt hammertest JCS estimation chart showing correlation between Schmidt hammer rebound number, hammer orientation, UCS, and rock density [52].

Table 1. Investigation sites, lithotypes, and survey types. X = measurement performed.

Site	Lithotype	Laser Scanner	I	Schmidt Hammer (r)	JRC
Monte Pellegrino	limestone	Riegl lms-Z210	X	X	
Monte Catalfano	limestone	Faro Focus 3D	X	X	X
PizzoLupo-Castronovo	limestone	Faro Focus 3D	X	X	
Latomiae del Paradiso	biocalcarenite	Leica Scan Station	X	X	
Palazzo Jung	ammonitic red limestone	Riegl lms-Z210	X	X	
Laboratory test	calcarenite, tuff	Faro Focus 3D	X	X	

Sites of investigation include various rock elements and rock outcrops in Sicily, Italy: the northwestern slope of Monte Pellegrino (Palermo), the walls of a quarry on the south slope of Monte Catalfano near Bagheria (Palermo), the walls of the cultivation area extending along the northeastern slope of PizzoLupo in Castronovo di Sicilia (Palermo), the ancient quarries of Latomia del Paradiso (Siracusa), and the ammonitic red limestone of Palazzo Jung in Palermo. Additionally, some data were obtained through laboratory measurements on calcarenite from foundation soils in Palermo and tuff from Naples. On these various lithotypes, surveys were conducted using both the laser scanner and the Schmidt hammer. It was observed that, in selected portions of the walls at these sites, there were areas characterized by different degrees of alteration. Additionally, it was noted that the reflectivity (*I*) varies considerably depending on the degree of alteration.

3. Results

3.1. Evaluation of Joint Wall Compressive Strength JCS

Survey 1. At Monte Pellegrino (Figure 2), the experimentation was conducted on the wall with an average inclination (α) of 81° and an azimuth of inclination (β) of 355° , situated

along an artificial trench (Monte Ercta) carved into Mesozoic limestone in the 1950s. The survey of the mesostructure, carried out using traditional techniques (scanlines and Clarr compass), terrestrial photogrammetry [53], and laser scanning, revealed the same oriented structure characterized by four main families of discontinuities. Two families (set 2 and set 4) have a “direction” sub-parallel to the wall, while the other two (set 1 and set 3) have a direction almost orthogonal to the trench. The surveys were conducted using the RIEGL LMS-Z210 laser scanner, featuring a scanning field of $80^\circ \times 360^\circ$. It is capable of measuring up to a distance of 486 m with a precision of 14 mm, using programmed angular steps. The acquisition speed can reach up to 9387 points/s, and the wavelength of the emitted beam is $1\mu\text{m}$. The laser scanner was positioned at a minimum distance of about 10m, and the scan was executed with a resolution of 0.018° . For reflectivity evaluations, a section of the wall was chosen where discontinuities coexist, exceeding 1m^2 in extent, with different types and degrees of alteration. On the discontinuities characterized by smooth surfaces in the upper portion (Figure 2a), which exhibit a corroded and vacuolar appearance near the roadbed, the measured values of reflectivity (I) range from 35% to 55%. The lower values ($I = 35\% \div 45\%$) are associated with fractured rock, resulting in the wall having pronounced small-scale roughness. Similar values were measured at the altered discontinuities with surfaces rendered rough due to the presence of pores and vacuoles. In the presence of altered but smooth surfaces with a uniform texture (Figure 2b), the measured values of I_m averaged approximately 47%. Intact and slightly altered rock (Figure 2c) provided an average I_m value of 52.5%. These measurements were compared with rebound values (r) obtained using the Schmidt hammer. In the zone dominated by fractured rock and on altered discontinuities with a corroded and vacuolar surface, the average rebound value (r_m) range is 31%. On altered discontinuities with a uniform surface, the average rebound value (r_m) is 42%. On slightly altered surfaces or massive rock, average rebound values (r_m) are 52%. In the first zone (fractured rock), it is highly likely that the results are influenced by the extremely variable volume of rock fragments on which the measurements were taken. As the value of I increases, there is also an observed increase in the rebound value (r).

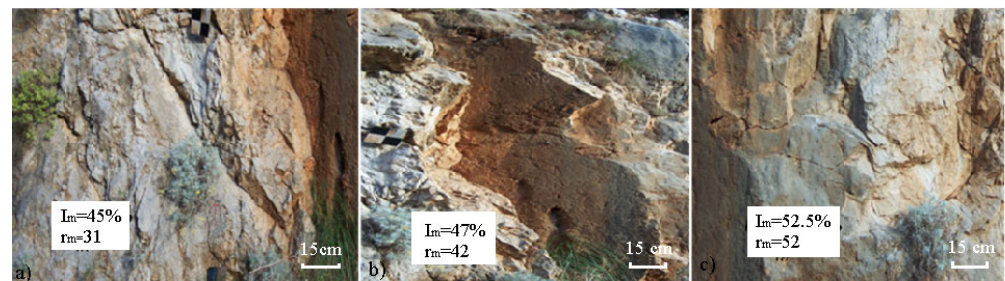


Figure 2. Monte Pellegrino: portions of the wall characterized by different degrees of alteration. Schmidt hammer estimations (r_m) and reflectivity measured by the laser scanner (I_m): (a) smooth surfaces (b) altered but smooth surfaces with a uniform texture (c) intact and slightly altered rock.

Survey 2. The second site chosen for a laser scanner survey is one of the abandoned quarries of dolomitic limestone located on Monte Catalano near Bagheria (Palermo) (Figure 3). The quarry face, measuring $10,000\text{m}^2$, has a height of 120m. Considering the technical specifications of the laser scanner, the morphology of the object to be scanned, and the features to be captured (meso-structural arrangement and roughness characteristics of the discontinuities), the scan points were planned to ensure a minimum overlap percentage of 30% between individual scans. The FARO FOCUS 3D laser scanner, with a scanning range of $305^\circ \times 360^\circ$ and the ability to measure up to a distance of 120 m with programmed step angles, was positioned approximately 15m away from the wall. The acquisition speed can reach up to 976,000 points/s. The emitted laser beam has a wavelength of 0.90 microns. For the necessary three-dimensional rendering of the surveys and subsequent roto-translation operations, it was planned that at least eight points on the wall would be recognizable in each capture.



Figure 3. Monte Catalfano: points cloud of rock mass collected using a laser scanner. Highlighting the seventy discontinuities from which the sections have been extracted.

To proceed with the comparison between the strength values measured using traditional direct techniques (Schmidt hammer) and those obtainable from the laser scanner survey, a section of the wall was selected. This section contains discontinuities with different types and degrees of alteration. On the 3D model, for each of the seventy discontinuities where rebound values (r) were measured, reflectivity values (I) were extracted from the point cloud returned by the laser scanner (Figure 4).



Figure 4. Monte Catalfano: Discontinuity 1–7 on the mesh in layer format reflectivity.

Reflectivity values (I) ranging between 30% and 56% were measured. The lower values ($30 \div 45$), with an average value $I_m = 39\%$ and generally more scattered, were associated with areas where the incident beam partially penetrates and scatters within micro-cavities, as in the case of corroded and vacuolar surfaces, or in the presence of very irregular surfaces due to flake detachment, or even at open discontinuities. On portions of discontinuities with altered but smooth surfaces, reflectance values (I) ranging between 53% and 56% were recorded, with generally less dispersion (Figure 5). For the Monte Catalfano lithotype as well, there is an observed increase in the average rebound value (r) with the growth of I , and the data appear to be correlated.

The lowest values of r and I are associated with the discontinuities (2) in Figure 5 characterized by significantly altered and highly fractured surfaces.

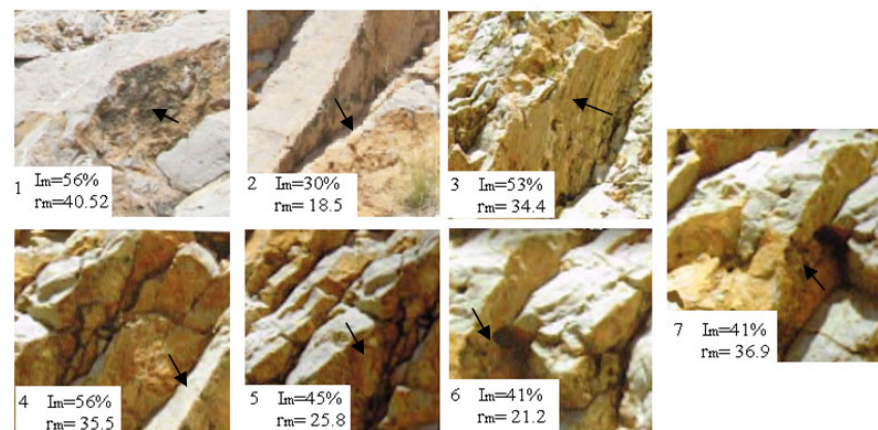


Figure 5. Photo of the seven discontinuities chosen for the assessment of rebound and reflectivity values. Discontinuity 1–7 of the Figure 4. The arrow indicates the portion of discontinuity investigated.

Survey 3. At the site of Castronovo di Sicilia, a rock mass exhibiting an overall west-dipping monocline, interrupted by two main fault systems—one oriented NW-SE and the other NE-SW—was investigated. These faults tend to intersect, leading to varying degrees of fragmentation of the structure, particularly in the southwestern sector where the quarry in question is located. For this site, the FARO FOCUS 3D laser scanner was used. For the scanning investigation describing the morphology of the subject and ensuring the necessary overlap, two station points were established within an area adjacent to the surveyed zone, avoiding shadow zones and areas of unclear identification. This approach allowed for scanning at a density of 1 point every 4mm, resulting in an overall collection of approximately 30 million points. This study was conducted by comparing the strength values measured using traditional direct techniques (Schmidt hammer) with those obtained from the survey through laser scanning in two specifically chosen zones (Zone 1 and Zone 2) within the quarry area (Figure 6). In Zone 1, near the alteration, an average reflectivity value (I_m) of 54.63% was measured, while in the area less affected by rock alteration, a mean reflectivity value (I_m) of 69.64% was observed. This analysis indicates that the zone characterized by alteration (Zone 1) exhibits lower average reflectivity values compared to those found in Zone 2. The average rebound value obtained on the wall identified in the first zone (Zone 1) is approximately (r_m) 19.75; in the area located a few meters away from the altered zone (Zone 2), we observed an average rebound value (r_m) of 41.1.

Survey 4. The ancient quarries of the Latomiae del Paradiso [54,55] are partially open-pit and partially underground. Reflectivity (I) measurements were conducted using the Leica Scan Station laser scanner, which has a scanning field of $360^\circ \times 270^\circ$. The acquisition speed can reach up to 4000 points/s, and the wavelength of the emitted ray (λ) is between 510 nm and 540 nm. The scan was performed with a density of 2 cm. The analysis of reflectivity measurements and their comparison with non-destructive investigations (e.g., Schmidt hammer) was conducted to validate the use of the laser scanner for morphological and topographical reconstruction and, as already presented for the other sites, also for zoning the rock's geomechanical conditions. The zoning is based on the characteristics of the rock wall surfaces, which, in a first approximation, can be distinguished into surfaces regularized due to mining and irregular surfaces characterized by fracture propagation (Figure 7). The zones of greater alteration are located below an aqueduct, orthogonal to the wall, where the weathering process was more intense, and phenomena of collapse and detachment of rock “flakes” had already occurred. The processing of reflectivity values (I), ranging between 37% and 58%, highlights the different levels of absorption of the rock. The lowest values, corresponding to the most intense weathering of the material, have been recorded in areas where the surface is uneven due to the collapse of the vault. The highest values correspond to areas regularized by mining. For these almost flat areas, the regularity of the walls has reduced the vulnerability of the material due to the lower specific surface

exposed to weathering agents. Rebound values (r) obtained from the Schmidt hammer range between 10 and 40.

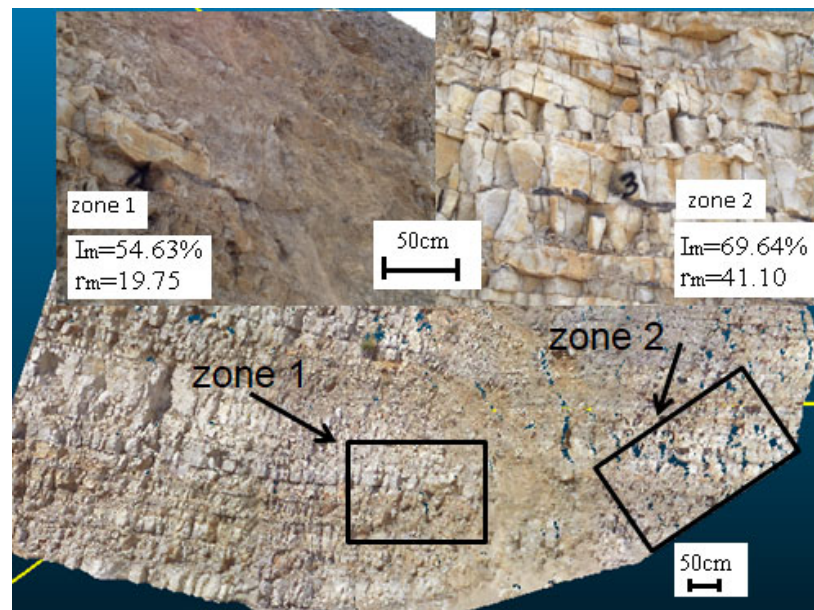


Figure 6. Castronovo di Sicilia. Chosen zones within the quarry area.



Figure 7. Latomie del Paradiso (Syracuse). Photo of the investigated area.

Survey 5. The research also focused on the study of the columns at the main entrance of Palazzo Jung in Palermo. The lithotype, ammonitic red limestone, characterized by a nodular and sometimes “flaser” structure, undergoes alterations when exposed to outdoor conditions, highlighting textural non-uniformities and, in severe cases, causing surface fractures [51]. The column on the right (see Figure 8) is prominently exposed to marine spray, resulting in signs of selective weathering that affect not only the chromatic appearance but also the rock’s state of aggregation. On the same column, different degrees of alteration can be observed depending on the orientation of the cylindrical surface to the marine spray. The column’s surface experiences a general whitening phenomenon, with intensity progressively increasing from areas facing the wall. The column exhibits the most altered band along a generatrix exposed to the east, towards the sea. For the altered column, the values of rebound (r) are dispersed in a wide range between 20 and 71. The surface of the altered column was divided into four vertical strips based on the visible level of alteration. The measured reflectivity values ranged between 45% and 55% (4 points in Figure 9). For the intact column (on the left), the reflectivity values ranged between 52% and 57% (1 point in Figure 9). The processed data further highlight the influence of the intensity of alteration on both the reflectivity values (I) and the rebound values (r) simultaneously.



Figure 8. Palazzo Jung (Palermo). Altered column (on the right) and intact column (on the left).

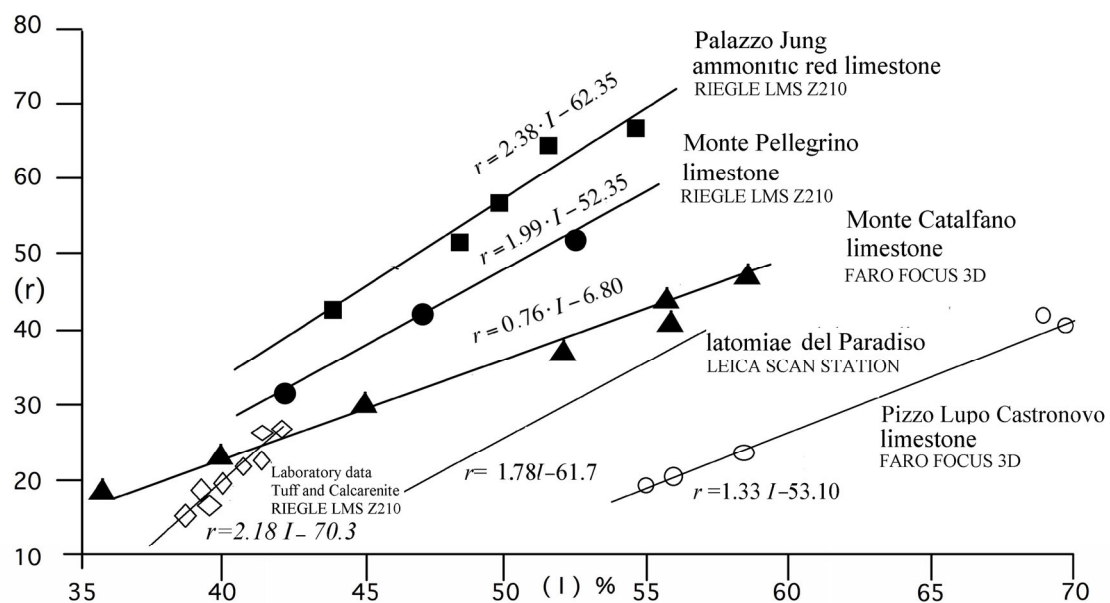


Figure 9. Relationships between reflectivity (I) and rebound (r) for the six surveys.

Survey 6. This study, conducted in the laboratory, focused on surveys (both direct and indirect) on tuff from Naples and calcarenite from Palermo. In laboratory investigations, for the indirect surveys, the RIEGL LMS-Z210 laser scanner, with a scanning field of $80^\circ \times 360^\circ$, was employed. Eight points were obtained (see Figure 9), highlighting the linear dependency of reflectivity (I) and rebound values (r). Regarding the Latomie del Paradiso, there are no experimental points because the line is obtained by interpolating average reflectivity and rebound data related to the zoning conducted on the rock mass based on the degree of alteration.

In the diagram in Figure 9, the relationships between average values of reflectivity (I) and rebound (r) for different lithotypes are compared. The figure displays data obtained from the six surveys performed on distinct lithotypes. From the overall analysis of the results, it can be concluded that the average values of the measurements obtained with the laser scanner are well correlated with those obtained with the Schmidt hammer. The figure also indicates the types of lasers used. Consequently, the parameters of the correlation curve depend on the wavelength of the beam emitted by the instrument and, essentially, on the model of the instrument used. The data were correlated using linear regression characterized by high values of the correlation coefficient ($R^2 = 0.93\text{--}0.98$). It is necessary to specify that the relationships obtained do not have absolute validity but undergo variations depending on the analyzed lithotype, as reflectivity is closely dependent on the type of

material constituting the surface subject to the survey. This is evident from the diagram in Figure 9, where the results obtained for different lithotypes are compared. The correlation between the spectral signatures and the strength of stone materials depends on the degree of alteration, which itself is influenced by various factors including chemical processes, environmental conditions, and humidity. In the context of rock mass characterization, operations are carried out under the same conditions to ensure accurate zoning of the rock mass.

Considering the relationship between reflectivity (I) and rebound (r) values, expressed as $r = mI + q$, Table 2 presents the values of m (angular coefficient) and q (intercept on the y -axis) for each lithotype. Furthermore, the table includes the rebound values corresponding to reflectivity values of 100% ($r_{I=100}$).

Table 2. Values of the slope coefficient (m) and the intercept (q) of the line for each lithotype.

Lithotype	m	q	$r_{I=100}$
Ammonitic red limestone (Palazzo Jung)	2.38	−62.35	176
Limestone (Monte Pellegrino)	1.99	−52.35	146
Limestone (Monte Catalfano)	0.76	−6.80	69
Limestone (PizzolupoCastronovo)	1.33	−53.10	80
Calcarenite (Latomie del Paradiso)	1.78	−61.7	116
Tuff and Calcarenite	2.18	−70.3	148

This study, conducted in the laboratory, included controlled weathering processes in samples of tuff and calcarenite to validate the correlation between reflectivity (I) and the degree of alteration. Tuff and calcarenite are two rocks that exhibit the typical mechanical behavior of hard soils/soft rocks. Two distinct techniques were employed to induce weathering processes: one based on the effects of thermal stress induced by repeated cycles of freezing (−20 °C) and thawing (+105 °C), and a second based on volume variations in anhydrous sodium sulfate during crystal formation. Tuff samples were subjected to freeze–thaw cycles, and both tuff and limestone samples were immersed in a saturated solution of sodium sulfate. In both lithotypes, a reduction in reflectivity was recorded as the material’s porosity (n) increased (Figure 10). The measurements provided variable values of reflectivity (I) within similar ranges for each lithotype, even in the presence of significantly different porosities. Schmidt hammer measurements were taken at the beginning and end of each weathering process. Similar to reflectivity (I) the values of rebound (r), regardless of the technique and lithotype, decreased with the progression of the weathering process, and the two parameters are correlated with linear regression.

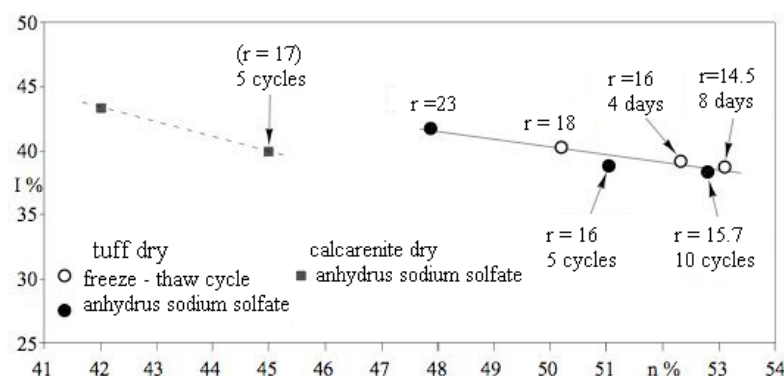


Figure 10. Influence of the decay of the texture on the reflectivity index (I) and the rebound values (r).

3.2. Evaluation of the Roughness of the Discontinuities and Joint Roughness Coefficient (JRC)

The morphology of surfaces, quantified by Barton using the Joint Roughness Coefficient (JRC), is one of the characteristics that govern the shear strength of discontinuities. JRC

can be obtained based on two options: roughness measurement in situ and in the laboratory based on the results of the direct shear test. In situ, it is typically assessed by measuring one or two profiles of the discontinuities in a specified direction with a profilometer, usually with dimensions up to 30–40 cm.

The obtained profile is then visually compared against typical profiles proposed by Barton and Choubey [56]. Nevertheless, there is a concern among researchers that the subjective nature of the visual comparison method could introduce biases in the *JRC* estimations. However, the limitation of this method lies in the length of the standard profiles compared to that of the entire joint, and the *JRC* parameter is significantly influenced by the scale effect. Barton [29] provides a precautionary method to account for this influence and to estimate the scale-corrected *JRC*. In this method, the value of *JRC* is obtained by correlating it with the inclination of the asperities (Figure 11a) [50]. The diagram (Figure 11b) is used to extrapolate the approximate *JRC* value of a discontinuity in Monte Catalfano (Figure 11c).

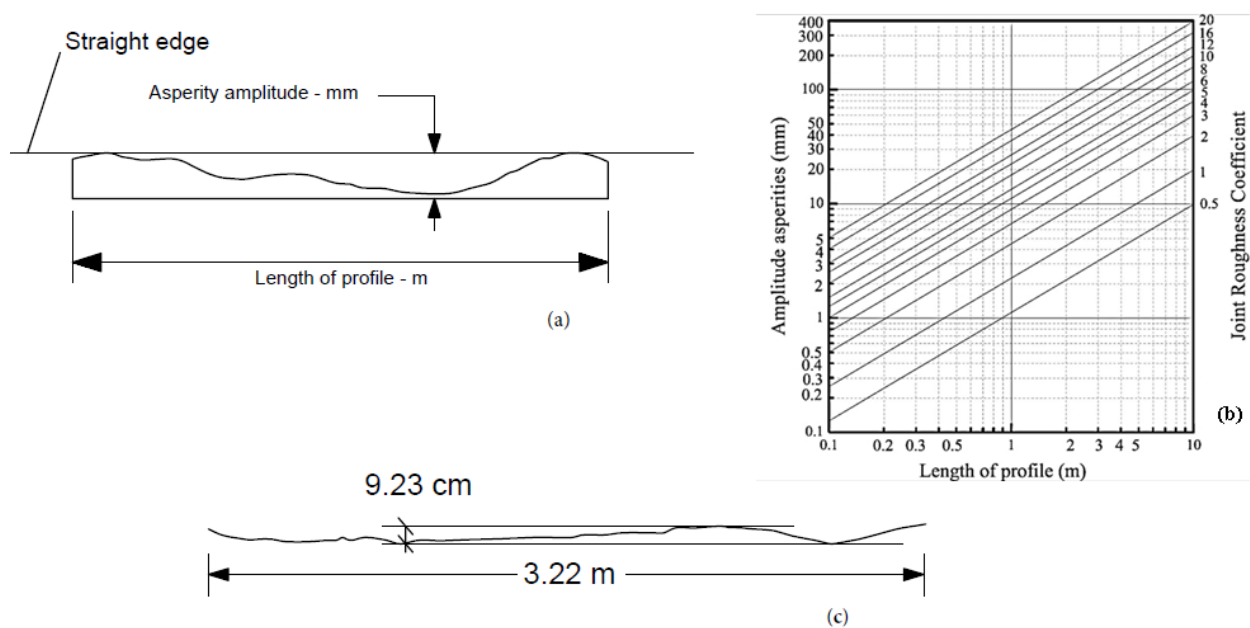


Figure 11. (a) Measurement of joint roughness amplitude, (b) diagram [29], and (c) example of measurement on a discontinuity in Monte Catalfano.

The anisotropy of surfaces [37], which is also a function of the genesis of the discontinuities themselves, cannot be considered with this method. In order to assess whether the laser technique overcomes these limitations, a more detailed evaluation of the anisotropy of roughness was developed on some discontinuities exposed on the wall of a quarry at Monte Catalfano. The additional advantage offered by the use of the laser scanner lies in the large number of obtainable coordinates, allowing for a statistical study of the inclinations of asperities as the base amplitude varies. This enables measurements in the direction of allowable kinematics.

To this end, each discontinuity surface has been sectioned with a series of planes normal to the surface itself. The first step was to identify on the mesh the plane containing the surface. For each discontinuity, three points were then identified on the mesh: the central point of the surface, i.e., the origin (O) of the plane being defined, and the endpoints of the *x* and *y* axes coinciding with the edges of the discontinuity. Care was taken to align the direction of one of the two axes (*x*, *y*) with the direction in which the surface develops most significantly. In order to assess the inclination (*i*) of asperities as their base amplitude varies in different directions, traces of sections between the plane of the discontinuities and a set of planes with axes orthogonal to the discontinuity were obtained. The planes in this set were inclined to each other at an angle of 30° (Figure 12). Following

the described procedure, 6 roughness profiles were thus obtained for each of the 70 selected discontinuities within the point cloud, resulting in a total of 420 profiles. On each roughness profile, the values of the inclination (i°) of asperities were measured as the base amplitude (a) varied in both opposite directions.

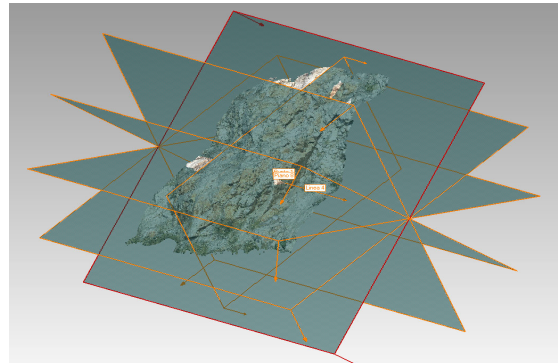


Figure 12. Bundle of planes with axis orthogonal to the discontinuity.

The results obtained indicate extreme variability in the angle of inclination (i°) as the base amplitude of the asperity varies and in the direction of the hypothesized kinematics (Figure 13). In particular, the inclination angle (i°) is maximum for asperities with small base amplitudes, similar to what is observable in laboratory tests, and it progressively tends to decrease for larger base amplitudes found on larger discontinuities. This result allows attributing, for a given direction, orientation, and a certain extent of the surface, an inclination angle (i°) value that is already corrected for the scale effect.

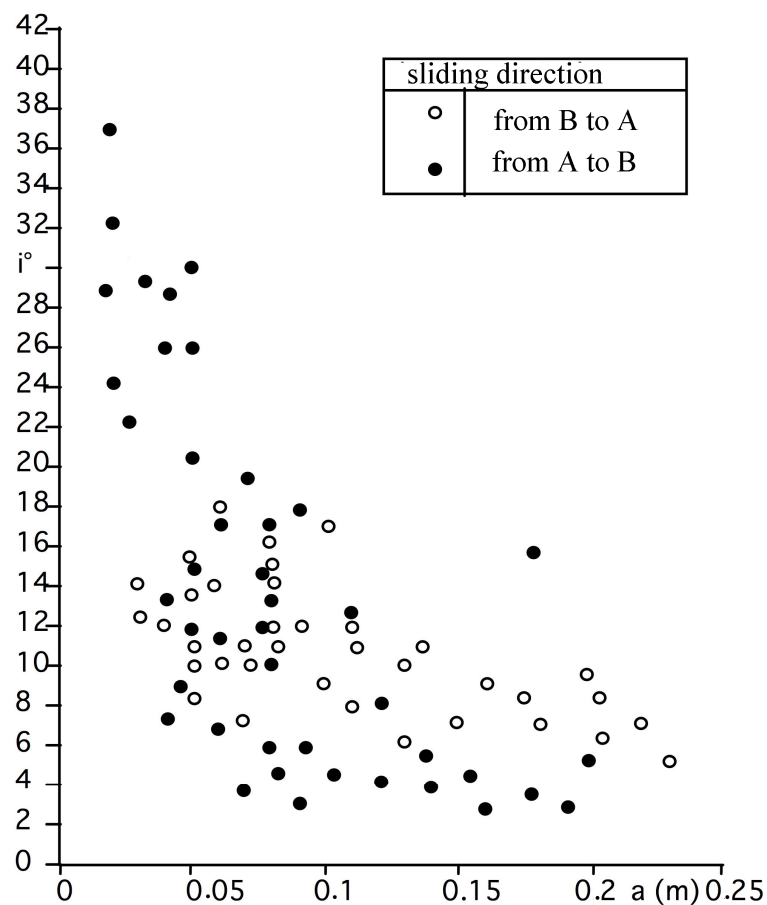


Figure 13. Inclination of asperity (i°)—base amplitudes (a): values measured on roughness profiles.

The processing of the profiles obtained, as described earlier, could replace the qualitative evaluation of Barton's Joint Roughness Coefficient (*JRC*). At a preliminary glance, this result, which requires further investigation, seems to challenge one of the assumptions of Barton's criterion, which proposes a single *JRC* value for a given profile, independent of the direction of kinematics.

4. Discussion

The conducted research highlights that investigations using laser scanners allow for the large-scale determination of the state of surface strength through reflectivity values (*I*), which are correlated to the Schmidt hammer rebound values (*r*). From the overall analysis of the results, it can be noted that the average values of measurements obtained with the laser scanner are well correlated with those obtained with the Schmidt hammer. This has allowed for the derivation of linear relationships correlating these two types of measurements (direct and indirect), thereby enabling the estimation of rebound values even for surfaces where direct measurement was not possible but indirect measurement can be carried out through the more convenient and effective laser scanning system. It is, however, worth noting that such linear correlations are obtainable for each individual rock mass (i.e., each lithotype) as reflectivity is closely dependent on the type of material composing the surface under survey. Through the linear correlation, any value of reflectivity measured in the comprehensive laser scanner survey can be associated with a rebound value. As a result, from these rebound values, it was possible to derive the Joint Coefficient of Strength (*JCS*), essential for determining shear strength using Barton's equation.

The results suggest that the laser scanner technique could be a useful tool for quantifying the state of alteration and, consequently, the strength of rock materials in a rapid and non-destructive manner, even over large areas. This method presents higher sensitivity than that achievable with the Schmidt hammer, not only because reflectivity measurement is carried out continuously over the entire investigated surface but also over extremely small areas, practically pixel-sized compared to the impact area of the Schmidt hammer piston. Additionally, the rebound value of the Schmidt hammer is influenced by the possible detachment of small portions of material around the impact surface. Through the geometric processing of coordinates acquired at a large number (10^6) of points on the surface of the discontinuity, it is possible to obtain roughness profiles in any direction and for the entire extent of the discontinuity. This allows for the reconstruction of textural anisotropy, particularly in directions of kinematically possible sliding or, more generally, on surfaces of project interest. This surpasses the limitations of *JRC* evaluation through a profilometer. An additional advantage provided by the use of the laser scanner is the ability to acquire a large number of coordinates, allowing for statistical analysis of the inclinations of asperities as the base amplitude varies. This, in turn, enables measurements in the direction of kinematically admissible sliding.

However, it is worth noting that the parameters of the correlation curve depend on the wavelength of the emitted beam from the instrument and, consequently, on the model of the instrument used. To make these correlations directly applicable, the research should include tracking the spectral signature of the specific rock mass under examination.

5. Conclusions

The analysis involved processing reflectivity measurements and comparing them with non-destructive techniques, such as the Schmidt hammer. This was performed to confirm the suitability of laser scanning not only for creating morphological and topographical reconstructions but also for zoning the rock geomechanical conditions. It is evident that the application of laser technology to the analysis of the shear behavior of discontinuities provides a substantial contribution to determining Barton parameters useful in detecting the strength of surfaces of discontinuities. The results of this research, therefore, have immediate practical implications for evaluating the in situ shear strength of discontinuities. With traditional techniques, the only option available for operators is to create a scan line

at the base of the cliff, thereby significantly restricting the evaluation of the entire rock face. Variations in properties along the rock face, at different heights, are usually assessed through rough and qualitative methods.

The dense acquisition of metric information through laser scans enables the assessment of multiple parameters (e.g., *JCR* and *JCS*), in contrast to traditional surveying techniques that necessitate a priori geometric and formal schematization and hierarchization. This establishes an initial interpretative model of space and serves as a guide in selecting the characteristic information to be acquired. The information density achievable through laser scanning allows for a continuous description of the geometry of the surveyed environmental portion.

In this research, it has been demonstrated how a simple 3D laser scanner can provide various information about the condition of the discontinuities. Through geometric processing of the acquired coordinates, which are numerous (approximately 10^6 points) on the surface of the discontinuity, it is possible to obtain roughness profiles in any direction and across the entire extent of the discontinuity. Consequently, the textural anisotropy can be reconstructed, particularly in the directions of kinematically possible sliding or, more generally, on surfaces of design interest. This effectively overcomes the limitations of *JRC* assessment through profilometer evaluation. Moreover, the overall results suggest that laser scanning could be a valuable method for quickly and accurately quantifying the alteration state of natural outcrops such as cliffs, slopes, or natural and artificial stone walls.

The laser scanner, through reflectance measurement, can provide quantitative assessments of the surface alteration phenomenon by measuring the reflectance of the surfaces of individual grains that make up the rock. Consequently, concerning the surface weathering state of the material, it exhibits much greater sensitivity than that achievable with the Schmidt hammer. This heightened sensitivity is attributed not only to the fact that reflectance measurement is carried out on much smaller surfaces than the impact area of the Schmidt hammer's piston but also because the rebound value of the hammer is influenced by the potential disconnection of small material portions in the volume surrounding the impact surface.

The results suggest that the laser scanner technique could be a useful tool for quantifying the state of alteration and, consequently, the strength of rock materials in a rapid and non-destructive manner, even over large areas, leading to a geomechanical zonation of the rock mass. Naturally, in every investigation, it will be necessary to establish the linear correlation between the values of the Schmidt hammer (r) and the reflectivity values (I) for each lithotype and rock mass studied. The instrument can be statistically validated when data correlating lithotype and alteration degree to rebound values are obtained without the measurement with the Schmidt hammer, as linear correlations valid for each class of lithotypes subjected to different degrees of alteration will be identified.

Author Contributions: Conceptualization, M.Z. and A.N.; Investigation, M.Z. and A.N.; Methodology, A.N., M.Z., and A.S.d.S.; Writing—original draft, A.N. and M.Z.; Writing—review and editing, A.N., M.Z., and A.S.d.S. All authors have read and agreed to the published version of the manuscript.

Funding: This research received no external funding.

Institutional Review Board Statement: Not applicable.

Informed Consent Statement: Not applicable.

Data Availability Statement: The data is contained within this article.

Acknowledgments: The authors would like to express their gratitude to Nicola Nocilla, whose valuable advice, counsel, and expertise significantly contributed to the research on the geomechanical characterization of rock masses.

Conflicts of Interest: The authors declare no conflicts of interest.

References

1. Kemeny, J.; Post, R. Estimating three-dimensional rock discontinuity orientation from digital images of fracture traces. *Comput. Geosci.* **2003**, *29*, 65–77. [\[CrossRef\]](#)
2. Kenner, R.; Phillips, M.; Danioth, C.; Denier, C.; Thee, P.; Zraggen, A. Investigation of rock and ice loss in a recently deglaciated mountain rock wall using terrestrial laser scanning: Gemsstock Swiss Alps. *Cold Reg. Sci. Technol.* **2011**, *67*, 157–164.
3. Singh, S.K.; Banerjee, B.P.; Raval, S. A review of laser scanning for geological and geotechnical applications in underground mining. *Int. J. Min. Sci. Technol.* **2023**, *33*, 133–154. [\[CrossRef\]](#)
4. Gigli, G.; Casagli, R. Semi-automatic extraction of rock mass structural data from high resolution LIDAR point clouds. *Int. J. Rock Mech. Min. Sci.* **2011**, *48*, 187–198. [\[CrossRef\]](#)
5. Sturzenegger, M.; Stead, D. Close-range terrestrial digital photogrammetry and terrestrial laser scanning for discontinuity characterization on rock cuts. *Eng. Geol.* **2009**, *106*, 163–182. [\[CrossRef\]](#)
6. Pagano, M.; Palma, B.; Ruocco, A.; Parise, M. Discontinuity Characterization of Rock Masses through Terrestrial Laser Scanner and Unmanned Aerial Vehicle Techniques Aimed at Slope Stability Assessment. *Appl. Sci.* **2020**, *10*, 2960. [\[CrossRef\]](#)
7. Umili, G. Ricostruzione automatica delle linee di rottura nei Modelli Digitali di Superficie con applicazioni in ambito geotecnico e architettonico. *Boll. Della Soc. Ital. Di Fotogram. E Topogr.* **2013**, *2*, 91–113.
8. Roncella, R.; Forlani, G. Extraction of planar patches from point clouds to retrieve dip and dip direction of rock discontinuities. Workshop 'Laser scanning 2005'. In Proceedings of the International Archives of the Photogrammetry, Remote Sensing and Spatial Information Sciences, XXXVI, Enschede, NL, USA, 12–14 September 2005; pp. 162–167.
9. Singh, S.K.; Banerjee, B.P.; Lato, M.J.; Sammut, C.; Raval, S. Automated rock mass discontinuity set characterisation using amplitude and phase decomposition of point cloud data. *Int. J. Rock Mech. Min. Sci.* **2022**, *152*, 105072. [\[CrossRef\]](#)
10. He, M.; Zhang, Z.; Deep, N.L. Convolutional Neural Network-Based Method for Strength Parameter Prediction of Jointed Rock Mass Using Drilling Logging Data. *Int. J. Geomech.* **2021**, *21*, 04021111. [\[CrossRef\]](#)
11. He, M.; Zhang, Z.; Yao, X.; Chen, Y.; Zhu, C. An empirical method for determining the mechanical properties of jointed rock mass using drilling energy. *Int. J. Rock Mech. Min. Sci.* **2019**, *116*, 64–74. [\[CrossRef\]](#)
12. Hazrathosseini, A.; Mahdevari, S. Geometric quality assessment of in situ blocks in dimension stone quarries. *Bull. Eng. Geol. Environ.* **2019**, *78*, 2377–2385. [\[CrossRef\]](#)
13. Hasan, M.; Shang, Y.; Shao, P.; Yi, X.; Meng, H. Evaluation of Engineering Rock Mass Quality via Integration Between Geophysical and Rock Mechanical Parameters. *Rock Mech. Rock Eng.* **2022**, *55*, 2183–2203. [\[CrossRef\]](#)
14. Lu, H.; Kim, E.; Gutierrez, M. A probabilistic Q-system using the Markov chain to predict rock mass quality in tunneling. *Comput. Geotech.* **2022**, *145*, 104689. [\[CrossRef\]](#)
15. Zhao, J. Joint surface matching and shear strength. *Int. J. Rock Mech. Min. Sci.* **1997**, *34*, 179–185. [\[CrossRef\]](#)
16. Schmidt, E. A non-destructive concrete tester. *Concrete* **1951**, *59*, 34–35.
17. Cargill, J.S.; Shakoor, A. Evaluation of empirical methods for measuring the uniaxial strength of rock. *Int. J. Rock Mech. Min. Sci.* **1990**, *27*, 495–503. [\[CrossRef\]](#)
18. Torabi, S.R. Reliability of the application of Schmidt hammer in determination of the UCS, Final project report. In *Persian*; Shahrood University of Technology: Shahrood, Iran, 2005.
19. González, J.A.; Rodríguez, B.R.; González, A.; Rivas-Brea, T.M. Terrestrial laser scanning intensity data applied to damage detection for historical building. *J. Archaeol. Sci. ISPRS J. Photogramm. Remote Sens.* **2010**, *37*, 3037–3047.
20. Franceschi, M.; Teza, G.; Preto, N.; Pesci, A.; Galgaro, A.; Girardi, S. Discrimination between marls and limestones using intensity data from terrestrial laser scanner. *ISPRS J. Photogramm. Remote Sens.* **2009**, *64*, 522–528. [\[CrossRef\]](#)
21. Johannsen, C.J.; Sanders, J.L. *Remote Sensing for Resource Management*; Soil Conservation Society of America: Ankeny, USA, 1982.
22. Jain, S.K.; Singh, V.P. *Water Resources Systems Planning and Management*; Baton Rouge: Los Angeles, CA, USA, 2003.
23. Dąbski, M.; Badura, I.; Kycko, M.; Grabarczyk, A.; Matlakowska, R.; Otto, J.-C. The Development of Limestone Weathering Rind in a Proglacial Environment of the Hallstätter Glacier. *Minerals* **2023**, *13*, 530. [\[CrossRef\]](#)
24. Singer, R.B. Spectral evidence for mineralogy of high-albedo soils and dust of Mars. *J. Geophys. Res.* **1982**, *87*, 10159–10168. [\[CrossRef\]](#)
25. Morris, R.V.; Agresti, D.G.; Lauer, H.V.; Newcomb, J.A.; Shelfer, T.D.; Murali, A.V. Evidence for pigmentary hematite on Mars based on optical, magnetic, and Mössbauer studies of supermagnetic (nanocrystalline) hematite. *J. Geophys. Res.* **1989**, *94*, 2760–2778. [\[CrossRef\]](#)
26. Barton, N. A relationship between joint roughness and joint shear strength. *Symp. Soc. Internat. Mec. Des Roches Nancy* **1971**, 1–8.
27. Fardin, N.; Stephansson, O.; Jing, L. The scale dependence of rock joint surface roughness. *Int. J. Rock Mech. Min. Sci.* **2001**, *38*, 659–669. [\[CrossRef\]](#)
28. Tse, R.; Cruden, D.M. Estimating joint roughness coefficients. *Int. J. Rock Mech. Min. Sci. Geomech. Abstr.* **1979**, *16*, 303–307. [\[CrossRef\]](#)
29. Bandis, S.; Lumsden, A.C.; Barton, N. Experimental Studies of Scale Effects on the Shear Behaviour of Rock Joints. *Int. J. Rock Mech. Min. Sci. Geomech. Abstr.* **1981**, *18*, 1–21. [\[CrossRef\]](#)
30. Du, S.G.; Fan, L.B. The statistical estimation of rock joint roughness coefficient Chin. *J. Geophys.* **1999**, *42*, 577–580.
31. Du, S.G.; Yun, J.H.; Xiao, F.H. Measurement of joint roughness coefficient by using profilograph and roughness ruler. *J. Earth Sci.* **2009**, *20*, 890–896. [\[CrossRef\]](#)

32. Tatone, B.S.A.; Grasselli, G. A new 2D discontinuity roughness parameter and its correlation with JRC. *Int. J. Rock Mech. Min. Sci.* **2010**, *47*, 1391–1400. [[CrossRef](#)]
33. Li, Y.; Huang, R. Relationship between joint roughness coefficient and fractal dimension of rock fracture surfaces. *Int. J. Rock Mech. Min. Sci.* **2015**, *75*, 15–22. [[CrossRef](#)]
34. Ficker, T.; Martisek, D. Alternative method for assessing the roughness coefficients of rock joints. *J. Comput. Civ. Eng.* **2016**, *30*, 04015059. [[CrossRef](#)]
35. Gravanis, E.; Pantelidis, L. Determining of the Joint Roughness Coefficient (JRC) of Rock Discontinuities Based on the Theory of Random Fields. *Geosciences* **2019**, *9*, 295. [[CrossRef](#)]
36. Liu, X.; Zhu, W.; Liu, Y.; Guan, K. Reconstruction of rough rock joints: 2D profiles and 3D surfaces. *Int. J. Rock Mech. Min. Sci.* **2022**, *156*, 105113. [[CrossRef](#)]
37. Attewell, P.B.; Farmer, I.W. *Principles of Engineering Geology*; Chapman and Hall: Boca Raton, FL, USA, 1977.
38. Fardin, N.; Feng, Q.; Stephansson, O. Application of a new in situ 3D laser scanner to study the scale effect on the rock joint surface roughness. *Int. J. Rock Mech. Min. Sci.* **2004**, *41*, 329–335. [[CrossRef](#)]
39. Ge, Y.; Tang, H.; Eldin, M.; Chen, P.; Wang, L.; Wang, J. A Description for Rock Joint Roughness Based on Terrestrial Laser Scanner and Image Analysis. *Sci. Rep.* **2015**, *5*, 16999. [[CrossRef](#)] [[PubMed](#)]
40. Re, F.; Scavia, C. Determination of contact areas in rock joints by X-ray computer Tomography. *Int. J. Rock Mech. Min. Sci.* **1999**, *36*, 883–890. [[CrossRef](#)]
41. Grasselli, G.; Wirth, J.; Egger, P. Quantitative three-dimensional description of a rough surface and parameter evolution with shearing. *Int. J. Rock Mech. Min. Sci.* **2002**, *39*, 789–800. [[CrossRef](#)]
42. Gaich, A.; Poetsch, M.; Fasching, A. Measurement of rock mass parameters based on 3D imaging. In Proceedings of the MIR 2004, X Ciclo di Conferenze di Meccanica e Ingegneria delle Rocce, Turin, Italy, 24–25 November 2004.
43. Mah, J.; Samson, C.; McKinnon, S.D.; Thibodeau, D. 3D laser imaging for surface roughness analysis. *Int. J. Rock. Mech. Min. Sci.* **2013**, *58*, 111–117. [[CrossRef](#)]
44. Scalco, L.; Tonietto, L.; Velloso, R.Q. Determination of roughness coefficient in 3D digital representations of rocks. *Sci. Rep.* **2022**, *12*, 10822. [[CrossRef](#)] [[PubMed](#)]
45. Grasselli, G. *Shear Strength of Rock Joints Based on Quantified Surface Description*; EPFL: Lausanne, Swiss, 2006.
46. Sadowski, L.; Czarnecki, S.; Hoła, J. Evaluation of the height 3D roughness parameters of concrete substrate and the adhesion to epoxy resin. *Int. J. Adhes. Adhes.* **2016**, *67*, 3–13. [[CrossRef](#)]
47. Tonietto, L.; Gonzaga, L.; Veronez, M.R.; Kazmierczak, C.D.S.; Arnold, D.C.M.; Costa, C.A.D. New Method for Evaluating Surface Roughness Parameters Acquired by Laser Scanning. *Sci. Rep.* **2019**, *9*, 15038. [[CrossRef](#)]
48. Bao, H.; Zhang, G.; Lan, H.; Yan, C.; Xu, J.; Xu, W. Geometrical heterogeneity of the joint roughness coefficient revealed by 3D laser scanning. *Eng. Geol.* **2020**, *265*, 105415. [[CrossRef](#)]
49. Wu, F.; Wu, J.; Bao, H.; Bai, Z.; Qiao, L.; Zhang, F.; Li, B.; Si, F.; Yu, L.; Guan, S.; et al. Rapid intelligent evaluation method and technology for determining engineering rock mass quality. *Rock Mech. Bull.* **2023**, *2*, 100038. [[CrossRef](#)]
50. Barton, N.; Wang, C.; Yong, R. Advances in joint roughness coefficient (JRC) and its engineering applications. *J. Rock Mech. Geotech. Eng.* **2023**, *15*, 3352–3379. [[CrossRef](#)]
51. Ercoli, L.; Megna, B.; Nocilla, A.; Zimbardo, M. Measure of a limestone weathering degree using Laser Scanner. *Int. J. Archit. Herit.* **2013**, *7*, 591–607. [[CrossRef](#)]
52. Deere, D.U.; Miller, R.P. *Engineering Classification and Index Properties for Intact Rock*; Air Force Weapons Laboratory Technical Report; National Technical Information Service: Springfield, VA, USA, 1966.
53. Aversa, S.; Nocilla, N.; Urcioli, G. Rilievi e analisi di ammassi a struttura orientata con la fotogrammetria terrestre. *Atti del GNCSIG del CNR* 1997.
54. Mastelloni, M.A.; Ercoli, L.; Nocilla, A.; Nocilla, N.; Sciortino, R.; Zimbardo, M. The Latomie of Syracuse: A Geotechnical Mapping through Rock Reflectivity. In *Engineering Geology for Society and Territory-Volume 8: Preservation of Cultural Heritage*; Lollino, G., et al., Eds.; Springer International Publishing: Berlin/Heidelberg, Germany, 2015; Volume 8.
55. Vitali, D.; Zimbardo, M.; Nocilla, A.; Ercoli, L.; Nocilla, N. Collapse Mechanisms in the Latomie of Syracuse (Sicily). *Riv. Ital. Di Geotec.* **2015**, *49*, 47–57.
56. Barton, N.; Choubey, V. The shear strength of rock joints in theory and practice. *Rock Mech.* **1977**, *10*, 1–54. [[CrossRef](#)]

Disclaimer/Publisher’s Note: The statements, opinions and data contained in all publications are solely those of the individual author(s) and contributor(s) and not of MDPI and/or the editor(s). MDPI and/or the editor(s) disclaim responsibility for any injury to people or property resulting from any ideas, methods, instructions or products referred to in the content.